Diagn Interv Radiol 2026; DOI: 10.4274/dir.2026.264280

INTERVENTIONAL RADIOLOGY

TECHNICAL NOTE

Arteriography- and portography-guided vascular mapping for clustered electrode placement in pancreatic irreversible electroporation

Man-Deuk Kim[1]
Joon Ho Kwon[1]
Jiwon Suk[2,3]
Seung Jeong[3,4]

[1]Yonsei University College of Medicine, Department of Radiology and Research Institute of Radiological Science, Seoul, South Korea

[2]Sogang University, Department of Electronic Engineering, Seoul, South Korea

[3]Medical Engineering Research Center, The Standard Co., Ltd, Gyeonggi-do, South Korea

[4]Seoul National University, Department of Biosystems Engineering, Seoul, South Korea

PURPOSE

To assess the feasibility, safety, and early imaging outcomes of an intraprocedural vascular mapping workflow integrating selective arteriography and/or portography to guide clustered electrode irreversible electroporation (IRE) for locally advanced pancreatic cancer (LAPC).

METHODS

In this single-center retrospective study, 48 patients with LAPC underwent percutaneous IRE (August 2024–December 2025). Selective arteriography (97.9%) and portography (75.0%) delineated the peripancreatic vascular anatomy. Clustered electrodes were supplemented as required. Technical success was defined as completion of the angiographic mapping workflow with planned electrode placement. The ablation zone-to-tumor size ratio was measured using intraprocedural computed tomography (CT) and early imaging response on the first follow-up CT.

RESULTS

The technical success rate was 100%. Selective arteriography was performed in 47/48 patients (97.9%) and portography in 36/48 (75.0%). Supplemented clustered electrode configurations were used in 44/48 patients (91.7%), and electrode repositioning was required in 3/48 (6.3%). Intraprocedural complications, both bleeding events, occurred in 2/48 patients (4.2%). Portal vein (PV) stent placement was performed in 11/48 patients (22.9%), with stent-related complications in 2/11 (18.2%)—one with systemic sepsis and one with PV thrombosis with intrahepatic extension. The ablation zone-to-tumor size ratio was ≥ 1.0 in all 48 patients (median, 1.29; range, 1.12–1.69). Imaging response was evaluable in 40/48 patients (83.3%) at a median of 85 days, with stable disease in 38/40 (95.0%) and progressive disease in 2/40 (5.0%).

CONCLUSION

Standardized vascular mapping supports consistent clustered electrode placement during pancreatic IRE in patients with LAPC, achieving complete ablation zone coverage in all patients.

CLINICAL SIGNIFICANCE

A standardized intraprocedural vascular mapping workflow using selective arteriography and portography supports reproducible clustered electrode placement during pancreatic IRE, achieving complete ablation zone coverage on intraprocedural CT in all cases and providing real-time anatomic guidance for safer electrode trajectory planning. This technical success provides a procedural framework for further evaluation of oncologic outcomes in prospective studies.

KEYWORDS

Irreversible electroporation, pancreatic cancer, arteriography, portography, vascular mapping, clustered electrode

Handling editor: Onur Taydaş

Corresponding author: Joon Ho Kwon

E-mail: golilla82@yuhs.ac

Received 07 July 2026; revision requested 23 July 2026; last revision requested 05 August 2026; accepted 06 August 2026.

Epub: 15.09.2026

DOI: 10.4274/dir.2026.264280

Irreversible electroporation (IRE) is a non-thermal ablation modality that has emerged as a promising treatment for locally advanced pancreatic cancer (LAPC), in which frequent abutment or encasement of major peripancreatic vessels often precludes resection and limits the safe application of thermal ablation techniques.[1-5] However, achieving consistent,

You may cite this article as: Kim MD, Kwon JH, Suk J, Jeong S. Arteriography- and portography-guided vascular mapping for clustered electrode placement in pancreatic irreversible electroporation. *Diagn Interv Radiol*. 15 September 2026 DOI: 10.4274/dir.2026.264280 [Epub Ahead of Print].

high-quality ablation with IRE remains technically challenging because outcomes depend on precise electrode alignment, adequate interelectrode distance, and geometric parallelism.[6,7] Inaccurate placement resulting in electrode convergence or divergence can reduce the effective ablation zone, generate excessive current, and compromise procedural safety and efficacy.

To mitigate these geometric constraints, clustered electrode designs with fixed interelectrode spacing have been developed.[8] Furthermore, LAPC frequently involves major vessels, and the peripancreatic vasculature serves as a critical anatomical reference for electrode trajectory planning. Compared with conventional ultrasound or static computed tomography (CT) guidance, integrated arteriography and portography provide dynamic, real-time delineation of the peripancreatic arterial and portal venous anatomy during electrode advancement, thereby improving intraprocedural spatial orientation and supporting safer electrode trajectory planning, particularly in cases with substantial vascular encasement. Although flush aortography has been used for real-time guidance, a standardized mapping protocol incorporating selective arteriography and portography has not been widely established as a reproducible workflow.[9]

The purpose of this study was therefore to evaluate the feasibility, periprocedural safety, and early imaging outcomes of a standardized intraprocedural vascular mapping workflow integrating selective arteriography and portography to guide clustered electrode placement during percutaneous IRE for LAPC.

Main points

- Intraprocedural vascular mapping using selective arteriography and portography enables consistent clustered electrode placement during percutaneous irreversible electroporation for locally advanced pancreatic cancer.
- Technical success was achieved in all 48 patients, with an ablation zone-to-tumor size ratio of ≥ 1.0 confirmed on intraprocedural computed tomography in all cases, indicating complete ablation zone coverage.
- This standardized workflow provides real-time anatomic guidance for electrode trajectory planning and may support safer procedural execution in complex peripancreatic cases near major vessels.

Methods

Study design and patient selection

This retrospective study was approved by the Institutional Review Board of Yonsei University Health System (decision/protocol number: 2026-1796-001, approval date: January 7, 2026), and the requirement for informed consent was waived. Between August 2024 and December 2025, 48 patients with LAPC who underwent percutaneous IRE were included. LAPC was defined as unresectable disease as determined by a multidisciplinary tumor board and based on institutional criteria. Patients were eligible for IRE if they were suitable candidates for general anesthesia, had a tumor measuring ≤ 4 cm, and had no ventricular cardiac arrhythmias. Exclusion criteria included distant metastasis, transmucosal invasion into adjacent gastrointestinal structures, uncontrolled infection, and severe comorbidities that precluded general anesthesia [e.g., Eastern Cooperative Oncology Group (ECOG) performance status ≥ 3, severe cardiopulmonary dysfunction, or end-stage organ failure]. The procedural workflow is illustrated in Figure 1.

Pre-procedural computed tomography review

Pre-procedural contrast-enhanced CT with arterial and portal venous phases and three-dimensional reconstructions was used to assess tumor–vessel relationships and plan electrode trajectories. Three-dimensional reconstructions were performed using TeraRecon Aquarius (TeraRecon Inc., Durham, NC, USA). Clustered electrodes with fixed interelectrode spacing (15, 17, or 20 mm) were selected to optimize tumor bracketing while avoiding direct vascular injury (Figures 2a–c, 3a). For pancreatic head lesions, a plastic biliary stent was endoscopically placed prior to imaging and IRE to prevent biliary obstruction and to serve as a non-conductive anatomical landmark.

Angiographic vascular mapping and direct portography

All procedures were performed in an integrated angiography–CT suite by two interventional radiologists with 10 and 21 years of experience in vascular and oncologic interventions. Selective angiography was performed via common femoral artery access to

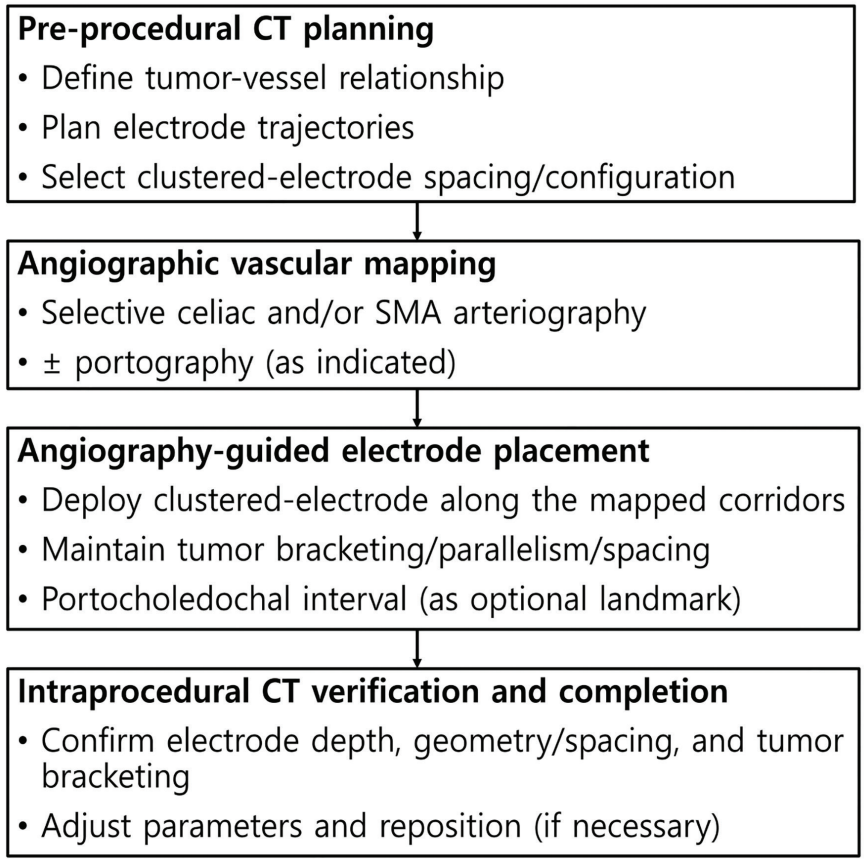

Figure 1. Procedural workflow. Intraprocedural vascular mapping workflow for angiography-guided clustered electrode placement for pancreatic irreversible electroporation. CT, computed tomography; SMA, superior mesenteric artery.

evaluate the peripancreatic arterial anatomy relevant to the planned electrode trajectories. Direct portography was selectively performed in cases with tumor-related venous narrowing and/or when planned trajectories were near the portal–splenic confluence. Under ultrasound guidance, a peripheral intrahepatic portal venous branch was accessed using a 21-G needle, followed by placement of a 5-F transhepatic sheath. Portography was performed using a 5-F catheter positioned at the superior mesenteric vein (SMV) confluence to delineate the portal venous anatomy and identify a safe insertion corridor (Figure 2d). When ultrasound-guided transhepatic access to a peripheral intrahepatic portal venous branch was not feasible because of inadequate visualization, small vessel caliber, or an unfavorable approach angle, indirect portography was performed using venous-phase imaging during selective superior mesenteric artery (SMA) angiography. Vascular mapping defined safe insertion corridors and provided real-time anatomic landmarks to verify electrode direction, spacing, and geometric parallelism. The fluoroscopy time, dose–area product, and total contrast volume were recorded for each case.

Portocholedochal interval

For descriptive purposes, the anatomic space between the common bile duct (identified by the plastic stent) and the PV is referred to as the "portocholedochal interval" (Figure 3b, c). This interval was carefully evaluated during vascular mapping to guide safe electrode trajectory planning, particularly in patients with pancreatic head tumors.

Electrode configuration and angiography-guided placement

All procedures used an EPO-IRE system with a generator and 18-gauge electrodes (The Standard Co., Ltd., Gunpo, South Korea). Electrode placement was performed under angiographic guidance following completion of vascular mapping. Clustered electrode configurations (double, trilateral triple, or square-shaped quadruple) were selected based on tumor morphology, with insertion trajectories optimized to maintain parallelism and avoid major perivascular landmarks. All clustered and single electrodes featured a 15-mm exposed tip length. For complex tumor geometries, standalone clustered electrodes were supplemented with additional electrodes to ensure complete bracketing and optimal alignment (Figures 2e, 3d). Subsequently, IRE was delivered at a target electric field strength of 1,500 V/cm (maximum, 3,000 V), 90 pulses per cycle, and a pulse width of 70–90 µs, with the voltage and pulse number adjusted according to intraprocedural current feedback. When minor geometric deviations were identified on intraprocedural CT, the voltage was reduced within the prespecified ceiling rather than proceeding with electrode repositioning.

To compensate for respiratory motion and roadmap shift, a microcatheter with a 0.014-inch guidewire was coaxially indwelled in the common hepatic, splenic, or SMAs to provide a stable anatomical reference. Final intraprocedural CT was performed to verify the electrode position, interelectrode spacing, and adequate tumor bracketing (Figure 2f).

Portal vein stent placement

Following ablation, follow-up arteriography and portography were performed to evaluate potential bleeding or thrombotic complications. Portal venous intervention was performed selectively when significant PV stenosis was identified, defined as ≥ 50% luminal narrowing with flow limitation and collateral venous pathways on portography. Bare-metal stents (10–12 mm, EPIC, Boston Scientific, MA, USA) were deployed across the target segment and post-dilated with balloons to restore patency. Before stent placement, 3,000 units of heparin were administered intravenously; subsequently, dual antiplatelet therapy with aspirin (100 mg) and clopidogrel (75 mg) was prescribed for 6 months to maintain stent patency. The transhepatic access tract was embolized using a vascular plug.

Outcomes and safety assessment

Angiographic mapping completion was defined as successful delineation of the relevant peripancreatic vascular anatomy through selective arteriography with direct or indirect portography when indicated. Technical success was defined as completion of the planned electrode placement in the intended configuration with adequate tumor bracketing confirmed on intraprocedural CT, following angiographic mapping completion. Procedural safety outcomes included intraprocedural and immediate post-procedural adverse events related to the vascular mapping and electrode deployment workflow.

Electrode geometric accuracy was assessed by the ablation zone-to-tumor size

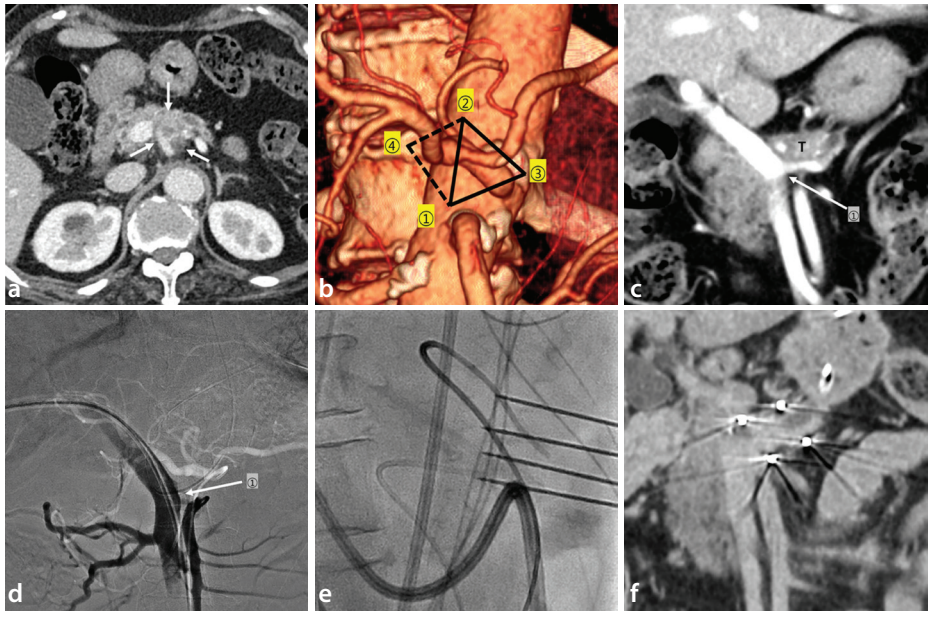

Figure 2. A 72-year-old woman with locally advanced pancreatic cancer. **(a)** Contrast-enhanced computed tomography (CT) shows a 1.8-cm mass in the pancreatic body (arrows), with encasement of the celiac trunk, common hepatic artery, and splenic artery and abutment of the main portal vein (PV). **(b)** Based on the tumor extent and its relationship to adjacent vascular structures, a combined configuration consisting of a triple clustered electrode with a 20-mm interelectrode spacing (1–3) and a single electrode (4) was planned. **(c)** The first electrode (1) of the triple clustered electrode configuration was targeted at the interval between the superior mesenteric artery and the main PV (arrow); the tumor **(T)** abutted the splenic vein and main PV. **(d, e)** Under combined arteriography and direct portography, all electrodes, including the first electrode (1), were placed with parallel alignment. **(f)** Verification by CT confirmed appropriate interelectrode spacing and adequate tumor bracketing. A follow-up CT obtained 7 months after IRE demonstrated stable disease (not shown), with a decrease in CA19-9 levels from 78 to 9.6 U/mL. IRE, irreversible electroporation; CA19-9, carbohydrate antigen 19-9.

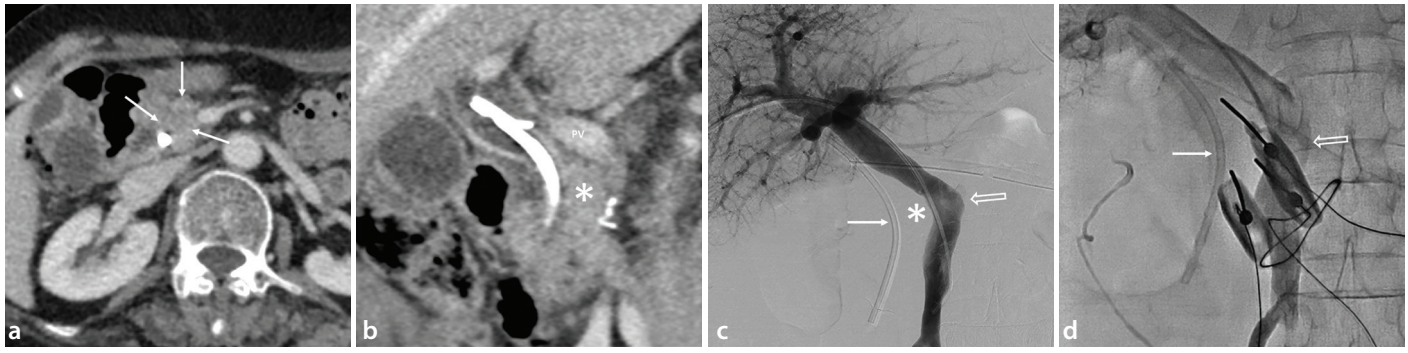

Figure 3. Portocholedochal interval. An 82-year-old woman with locally advanced pancreatic cancer. **(a)** Contrast-enhanced computed tomography (CT) shows a 2.0-cm mass in the pancreatic head. **(b)** Coronal CT depicts the portocholedochal interval (*), defined as the anatomical interval between the common bile duct (represented by a plastic biliary stent) and the portal vein (PV). **(c)** Direct portography further delineates the portocholedochal interval (*) between the plastic stent (arrow) and PV (open arrow). **(d)** A double clustered electrode configuration with an additional single electrode was inserted under fluoroscopic guidance. The plastic biliary stent (arrow) and contrast opacification of the PV (open arrow) are visible.

ratio (maximum ablation zone diameter on intraprocedural CT divided by maximum tumor diameter on pre-procedural CT); a ratio of ≥ 1.0 was defined as adequate coverage. Early imaging response was evaluated by a radiologist blinded to procedural details and clinical status using Response Evaluation Criteria in Solid Tumors (RECIST) version 1.1 on the first available follow-up contrast-enhanced CT. Patients without follow-up imaging and those in whom the ablation zone margin was indistinguishable from the surrounding pancreatic parenchyma on follow-up CT were classified as non-evaluable.

Statistical analysis

Continuous variables are expressed as mean ± standard deviation or median with range, as appropriate. Categorical variables are expressed as frequencies and percentages. All statistical analyses were performed using SPSS software (version 29.0; IBM Corp., Armonk, NY, USA).

Table 1. Baseline patient and tumor characteristics (n = 48)

Characteristics	Value
Patient characteristics	
Age (years), mean ± SD	64.8 ± 9.6
Sex, men/women, n (%)	25 (52.1%) / 23 (47.9%)
ECOG performance status, n (%)	
0	5 (10.4)
1	41 (85.4)
2	2 (4.2)
CA 19-9 at baseline (U/mL), median (range)	148.6 (1.5–7,257.6)
Prior systemic chemotherapy, n (%)	45 (93.8)
Concurrent systemic chemotherapy, n (%)	44 (91.7)
Tumor characteristics	
Location, n (%)	
Head	23 (47.9%)
Body	24 (50.0%)
Head and body (non-contiguous lesion)	1 (2.1%)
Size, max diameter (cm), mean ± SD (range)	2.9 ± 0.7 (1.5–4.0)

SD, standard deviation; ECOG, Eastern Cooperative Oncology Group; CA 19-9, carbohydrate antigen 19-9.

Results

Patient demographics and baseline tumor characteristics are summarized in Table 1. The majority of patients had ECOG performance status 1 (41/48, 85.4%), and prior systemic chemotherapy had been administered in 45/48 patients (93.8%). The median baseline carbohydrate antigen 19-9 level was 148.6 U/mL (range, 1.5–7,257.6).

Angiographic vascular mapping and electrode configuration strategy

Angiographic mapping completion and technical success were both achieved in all 48 patients (100%). Based on the mapping technique, arteriography alone was used in 12/48 patients (25.0%), combined arteriography with direct portography in 33/48 patients (68.8%), combined arteriography with indirect portography in 2/48 patients (4.2%), and direct portography alone in 1/48 patients (2.1%) (Table 2). The median fluoroscopy time was 18.0 min (range, 8.7–62.9), and the median radiation dose was 1,127.3 mGy·cm^2 (range, 652.2–2,848.8) in 27/48 patients for whom dosimetry data were available. The median contrast volume was 90 mL (range, 20–160).

Clustered electrode configurations ranged from standalone to supplemented designs, including double, triple, or quadruple configuration, to optimize tumor bracketing and geometric parallelism (Table 3). Standalone clustered electrode placement was performed in 4/48 patients (8.3%), whereas supplemented clustered configurations were used in 44/48 patients (91.7%).

Computed tomography verification and geometric accuracy

Intraprocedural CT was used to verify electrode positioning, interelectrode geometry, and tumor bracketing, and findings were consistent with those of angiographically guided corridors. Minor geometric deviations from the intended spacing (mild convergence or divergence) were typically managed by voltage adjustments rather than repositioning. Additionally, CT facilitated assessment of electrode depth, allowing for minor adjustments to optimize tumor coverage. Electrode repositioning was required in 3/48 patients (6.3%), most commonly involving single-electrode configurations. The portocholedochal interval served as a key landmark for electrode trajectory planning in 4/23 patients with pancreatic head tu-

mors. The ablation zone-to-tumor size ratio was ≥ 1.0 in all 48 patients, with a median of 1.29 (range, 1.12–1.69), indicating adequate tumor coverage in all cases.

Procedural safety

Complications occurred in 2/48 patients (4.2%), both of which were bleeding events detected on post-ablation angiography performed immediately after IRE. One patient developed active gastroduodenal artery (GDA) bleeding, which was successfully managed with glue embolization during the same session. In the other patient, bleeding from a dilated gastroepiploic varix was controlled with manual compression applied for approximately 10 minutes. In one uncinate process tumor, splenic vein transgression was necessary to achieve optimal electrode positioning. To mitigate thrombotic risk, 3,000 units of intravenous heparin were administered prior to IRE, and no thrombotic complications occurred during follow-up.

Outcomes of portal venous intervention

Adjunctive PV stent placement was performed in 11/48 patients (22.9%) to achieve immediate restoration of venous patency. Among the 11 patients who received PV stents, stent-related complications occurred in 2 (18.2%). In one patient, fever developed on postprocedural day 5, with gram-negative rod bacteremia on blood cultures. Follow-up CT demonstrated an abscess at the ablation site with a fistulous communication to the PV stent, suggesting translocation of organisms through the ablation–portal venous fistula as the source of systemic sepsis. Management included percutaneous catheter drainage of the abscess and transhepatic portal venous occlusion using a vascular plug to interrupt the hematogenous route, followed by clinical recovery. In another patient, postprocedural CT demonstrated PV thrombosis extending into the intrahepatic branches. This was managed with systemic anticoagulation therapy, and the thrombus remained stable under ongoing medical management.

Early imaging response

Early imaging responses are summarized in Table 4. Follow-up CT was available for 42/48 patients (87.5%); 6 (12.5%) had no follow-up imaging. Of the 42 patients with CT, 2 (4.2%) were non-evaluable due to an indistinct ablation zone margin; RECIST 1.1 was therefore evaluable in 40/48 patients (83.3%) at a median follow-up of 85 days (range, 11–140). Stable disease was achieved in 38/40 patients (95.0%) and progressive disease in 2/40 (5.0%). Among the patients with stable disease, the median tumor size change was +3.2% (range, −26.9 to +18.8%). The overall median tumor size change was +3.3% (range, −26.9 to +30.8%).

Table 2. Intraprocedural angiographic mapping techniques and procedure details

Variables	Value
Road-mapping technique, n (%)	
Arteriography alone	12 (25.0 %)
Combined arteriography and direct portography	33 (68.8%)
Combined arteriography and indirect portography	2 (4.2%)
Direct portography alone	1 (2.1%)
Procedure details, median (range)	
Fluoroscopy time (min)	18.0 (8.7–62.9)
Radiation dose, DAP (mGy·cm^2)	1,127.3 (652.2–2,848.8)
Contrast volume (mL)	90 (20–160)

DAP, dose-area product.

Table 3. Distribution of clustered and supplemented electrode configurations

Electrode configuration	No. of patients (%)
Standalone mode	
Quadruple only	3 (6.3%)
Triple only	1 (2.1%)
Supplemented clustered[a]*	
Quadruple-based with additional electrodes[b]†	18 (37.5%)
Double-based with additional electrodes[c]‡	16 (33.3%)
Triple-based with additional electrodes[c]‡	10 (20.8%)
Total	48 (100%)

a*Clustered electrodes were used as the primary backbone for electrode placement.
b†Supplemented with triple, double, or single electrodes.
c‡Supplemented with double or single electrodes.

Table 4. Early imaging responses (RECIST 1.1)

Variable	Value
RECIST 1.1 evaluable, n (%)	40 (83.3)
Follow-up interval, median (range), days	85 (11–140)
RECIST 1.1 response, n (%)	
Stable disease	38/40 (95.0)
Progressive disease	2/40 (5.0)
Median tumor size change, % (range)	+3.3 (−26.9 to +30.8)

RECIST, Response Evaluation Criteria in Solid Tumors.

Discussion

IRE remains technically demanding for LAPC, with broader adoption limited by the complexity of achieving reproducible electrode geometry within the constrained peripancreatic space.[10-12] Prior studies have emphasized that stable interelectrode spacing and true parallel alignment are among the most challenging technical components of pancreatic IRE.[13-15] This report describes a structured intraprocedural vascular mapping workflow that supports planning and verification of the clustered electrode trajectory.

A practical advantage of this approach is the use of the peripancreatic vasculature as an anatomic framework to define safe insertion corridors and avoid critical vascular structures during electrode advancement. Selective arteriography delineated the celiac axis, SMA, and pancreaticoduodenal arterial arcades to identify arterial structures and guide safe electrode advancement. When performed, portography provided detailed PV–SMV anatomy that was incorporated into trajectory planning. Indirect portography was used in two patients (4.2%) when transhepatic direct portography was technically challenging; however, direct portography

was used preferentially when feasible because it provided more detailed delineation of the portal venous anatomy. In addition, the plastic biliary stent provided a useful practical landmark for anatomic orientation and electrode depth assessment.

Based on vascular anatomy and tumor morphology, clustered electrode configurations, including double, triple, and square-shaped quadruple designs, were selected to achieve adequate tumor coverage. Clustered electrodes served as the primary backbone for electrode placement, and supplemented electrodes were added as needed to accommodate irregular tumor geometry while maintaining tumor bracketing, parallelism, and the intended interelectrode spacing throughout the procedure. Intraprocedural CT verification was used to assess electrode depth and to confirm electrode positioning. Minor deviations from the intended spacing (mild convergence or divergence) were typically managed by adjusting treatment parameters rather than by electrode repositioning, which was required in 3 patients (6.3%). The ablation zone-to-tumor size ratio was ≥ 1.0 in all 48 patients (median, 1.29; range, 1.12–1.69), indicating consistent and adequate tumor coverage throughout all procedures.

We propose the portocholedochal interval, defined as the anatomical space between the common bile duct (identified by a plastic biliary stent) and PV, as a pragmatic landmark for electrode trajectory planning in selected pancreatic head tumors. In the present study, this interval served as a key landmark in 4/23 pancreatic head tumors. Although not universally applicable, when integrated with angiographic mapping, it may provide an additional spatial cue in selected cases, supporting spatial orientation and electrode trajectory planning and potentially reducing the need for repeated electrode repositioning. This landmark appeared most consistently identifiable in patients with pancreatic head tumors in whom a plastic biliary stent had been placed prior to the procedure, providing clear fluoroscopic visualization of the bile duct, and in whom the PV was adequately delineated on portography. Cases with significant tumor encasement of the PV or with tortuous biliary anatomy may be less suitable for this approach.

Safety considerations are paramount in pancreatic IRE. Given complication rates of up to 58% reported in the literature, such technical refinements are essential.[9,16] In the present study, two bleeding complications were identified on post-ablation angiography and were promptly managed using endovascular or conservative measures. In one case of arterial bleeding, the electrode trajectory was adjacent to an indwelling metallic biliary stent that could not be removed. Although causality cannot be established, proximity to metallic hardware may plausibly influence local electric field behavior during high-voltage pulse, potentially leading to unintended energy concentration and thermal-mediated vascular injury to the adjacent GDA.[3] Metallic implants with high electrical conductivity can locally distort the applied electric field during IRE pulse delivery, leading to field concentration at the metal–tissue interface. This phenomenon, analogous to the "tip effect" described in radiofrequency ablation near metallic objects, may result in unintended joule heating and thermal injury to adjacent structures even in a nominally non-thermal modality such as IRE.[17] These physical considerations should inform electrode trajectory planning when metallic implants are present in the procedural field. In another case, venous bleeding originating from a gastroepiploic varix along the unavoidable electrode trajectory was identified and controlled with manual compression. The ability to detect and manage vascular injuries immediately represents a practical advantage of real-time angiography within this vascular mapping workflow.

Adjunctive portal venous management introduces additional risk–benefit considerations. Portal vein (PV) stenting was performed selectively in 11 patients, with the primary goal of maintaining vascular patency against tumor encasement and postprocedural edema. However, stent-related complications occurred in 18.2% (2/11) of patients with stents, including one case of systemic sepsis and one case of PV thrombosis with intrahepatic extension. These findings suggest that concurrent PV stenting during pancreatic IRE should be undertaken cautiously, with strict selection criteria and standardized postprocedural management. Potential selection criteria may include hemodynamically significant PV/SMV narrowing of at least 50% with impaired venous flow or collateral formation, absence of complete portal venous occlusion, and adequate hepatic functional reserve. Future studies should clarify the optimal timing and indications for portal venous intervention and determine whether staged strategies can reduce device-related risks without compromising venous patency.

It is also important to acknowledge the additional procedural burden of the vascular mapping workflow compared with conventional CT-guided IRE. Combined arterial and transhepatic portal venous catheterization may increase fluoroscopy time, radiation exposure, and contrast use and carries access-related risks, including bleeding and PV thrombosis. However, without a direct comparison group, the incremental burden attributable specifically to the mapping workflow could not be determined. Whether these additional procedural requirements provide sufficient technical or safety benefit should be evaluated in prospective comparative studies.

Early imaging response assessed by RECIST 1.1 showed stable disease in 95.0% of evaluable patients at a median of 85 days after IRE. The modest median tumor size change observed in patients with stable disease (+3.2%) likely reflects early ablation zone edema rather than true tumor progression, a pattern well documented in the IRE literature.[9] The two patients with progressive disease showed substantially larger size increases (+30.8% and +29.2%), consistent with the biological aggressiveness of LAPC. Notably, 2/40 evaluable patients (5.0%) demonstrated progressive disease on early imaging, underscoring the biological aggressiveness of LAPC and the need for concurrent systemic therapy. The two non-evaluable patients with an indistinct ablation zone margin may also represent a favorable response, as complete tumor–parenchyma boundary obliteration has been described after successful IRE.[3] These early imaging findings were intended to provide an exploratory assessment of early treatment response; however, given the limited follow-up period, they should not be interpreted as definitive evidence of durable oncologic efficacy or long-term local tumor control.

This study has several limitations. First, its retrospective, single-center design and the absence of a comparison group limit generalizability and preclude conclusions regarding the incremental benefit of vascular mapping over CT-only guidance. Selection bias is also possible because the decision to use the vascular mapping workflow was made at the discretion of the operating physicians. Patients considered technically suitable for this approach may therefore have been preferentially selected, potentially contributing to the observed 100% technical success rate. A prospective study with prespecified eligibility criteria and a comparator group is needed to address this limitation. Second, the follow-up period was insufficient to assess local tumor progression or survival, which will be

evaluated in subsequent analyses. Third, the sample size of 48 patients was not based on a formal power calculation, as this study was designed as a feasibility and safety evaluation rather than an efficacy trial; the cohort size is nonetheless comparable to other published feasibility studies on percutaneous IRE for LAPC, including prospective single-arm series of similar scale. Finally, the results reflect the experience of a high-volume center with expertise in combined angiography–CT procedures and may not be generalizable to centers with less experience or to patients with more extensive vascular encasement or limited transhepatic access. In such anatomically challenging cases, the mapping strategy and criteria for technical success may require modification.

In conclusion, standardized intraprocedural vascular mapping offers a practical workflow for consistent clustered electrode placement during pancreatic IRE in patients with LAPC, achieving complete ablation zone coverage in all patients. It should be noted that complete ablation zone coverage on intraprocedural imaging does not necessarily equate to complete tumor necrosis or guarantee long-term local tumor control, and prospective studies with oncologic endpoints are needed to establish the clinical benefit of this approach.

Footnotes

Conflict of interest disclosure

Man-Deuk Kim serves as a consultant for Standard Co., Ltd. Jiwon Suk and Seung Jeong are affiliated with Standard Co., Ltd, but declare no competing financial interests related to this work. The company provided the EPO-IRE devices and technical support but had no role in study design, patient selection, data collection, data analysis, or interpretation of the results. The remaining authors declare no conflict of interest.

Funding

This work was supported by "Supporting Project to Clinical evaluation Domestic Medical Devices in Hospitals" funded by "Ministry of Health and Welfare (MOHW)" and "Korea Health Industry Development Institute (KHIDI)".

References

1. Martin RC 2nd, McFarland K, Ellis S, Velanovich V. Irreversible electroporation therapy in the management of locally advanced pancreatic adenocarcinoma. *J Am Coll Surg*. 2012;215(3):361-369. [Crossref]
2. Bergenfeldt M. The role of irreversible electroporation (IRE) for locally advanced pancreatic cancer: a systematic review of safety and efficacy. *Scand J Gastroenterol*. 2017. [Crossref]
3. Aycock KN, Davalos RV. Irreversible electroporation: background, theory, and review of recent developments in clinical oncology. bioelectricity. 2019;1(4):214-234. [Crossref]
4. Linecker M, Pfammatter T, Kambakamba P, DeOliveira ML. Ablation strategies for locally advanced pancreatic cancer. *Dig Surg*. 2016;33(4):351-359. [Crossref]
5. Young SJ. Irreversible electroporation and the pancreas: what we know and where we are going? *World J Gastrointest Surg*. 2015;7(8):138-144. [Crossref]
6. Martin RC, Schwartz E, Adams J, Farah I, Derhake BM. Intra - operative anesthesia management in patients undergoing surgical irreversible electroporation of the pancreas, liver, kidney, and retroperitoneal tumors. *Anesth Pain Med*. 2015;5(3):e22786. [Crossref]
7. Dunki-Jacobs EM, Philips P, Martin RC 2nd. Evaluation of resistance as a measure of successful tumor ablation during irreversible electroporation of the pancreas. *J Am Coll Surg*. 2014;218(2):179-187. [Crossref]
8. Kwon JH, Kim MD, Alanazi MS, et al. Prospective evaluation of irreversible electroporation with clustered electrodes as a novel palliative approach for locally advanced pancreatic cancer. *Korean J Radiol*. 2026;27(2):152-160. [Crossref]
9. Ruarus AH, Vroomen LGPH, Geboers B, et al. Percutaneous Irreversible electroporation in locally advanced and recurrent pancreatic cancer (PANFIRE-2): a multicenter, prospective, single-arm, phase II study. *Radiology*. 2020;294(1):212-220. [Crossref]
10. Martin RC 2nd, Durham AN, Besselink MG, et al. Irreversible electroporation in locally advanced pancreatic cancer: a call for standardization of energy delivery. *J Surg Oncol*. 2016;114(7):865-871. [Crossref]
11. Narayanan G. Irreversible electroporation. *Semin Intervent Radiol*. 2015;32(4):349-355. [Crossref]
12. Fang C, Kibriya N, Heaton ND, et al. Safety and efficacy of irreversible electroporation treatment in hepatobiliary and pancreatic tumours: a single-centre experience. *Clin Radiol*. 2021;76(8):599-606. [Crossref]
13. Latouche EL, Sano MB, Lorenzo MF, Davalos RV, Martin RCG 2nd. Irreversible electroporation for the ablation of pancreatic malignancies: a patient-specific methodology. *J Surg Oncol*. 2017;115(6):711-717. [Crossref]
14. Rao S, Bui TL, Sasani A, et al. Irreversible electroporation for pancreatic cancer using intraprocedural cone-beam computed tomography fusion navigation: a case report. *J Med Case Rep*. 2021;15(1):566. [Crossref]
15. Fang G, Niu L, Chen J. Prevention of procedural hypertension in the irreversible electroporation ablation of liver and pancreatic tumors based on distance from the adrenal gland. *Cancer Manag Res.* 2020;12:71-78. [Crossref]
16. Tasu JP, Herpe G, Damion J, et al. Irreversible electroporation to bring initially unresectable locally advanced pancreatic adenocarcinoma to surgery: the IRECAP phase II study. *Eur Radiol*. 2024;34(10):6885-6895. [Crossref]
17. Scheffer HJ, Vogel JA, van den Bos W, et al. The influence of a metal stent on the distribution of thermal energy during irreversible electroporation. *PLoS One*. 2016;11(2):e0148457. [Crossref]